1st LATAM-SHM 2023 Conference
A. Güemes, L. Mujica, J. Sierra (Eds)

GUIDED WAVE-BASED DAMAGE IMAGING OF QUARTZ CERAMIC THERMAL PROTECTION STRUCTURES ABLATION

HUI ZHENG, FAN SHAO, QIDI SHAN, LEI QIU†, SHENFANG YUAN†

† Research Center of Structural Health Monitoring and Prognosis
State Key Laboratory of Mechanics and Control for Aerospace Structures
Nanjing University of Aeronautics and Astronautics
Nanjing210016, P. R. China
Email: lei.qiu@ nuaa.edu.cn
Email: ysf@ nuaa.edu.cn

Key words: Guided wave; Quartz ceramic; Thermal protection structures; Damage imaging; Hypersonic vehicle.

Abstract. As a key protective component for hypersonic vehicle in harsh service environment, the thermal protection structure (TPS) is prone to ablation damage in the extreme thermal environment during the reentry process of the vehicle, seriously affecting its safe service, and structural health monitoring (SHM) is urgently needed. In this paper, the delay-and-accumulation damage imaging method based on guided wave (GW) is used to study the damage imaging of the ablation damage of the quartz ceramic TPS structure. First, the ablation damage of the quartz ceramic TPS structure was produced by oxygen-acetylene high-temperature and high-speed gas flow ablation, and then a GW monitoring experiment method for the ablation of the quartz ceramic TPS was designed, and the results of the quartz ceramic TPS under different states and different damage degrees were obtained. Finally, by extracting the GW signal features in different states and different damage degrees, the delay-and-accumulation imaging method is used to image and locate the ablation damage of quartz ceramics. The results show that the delay-and-accumulation imaging algorithm based on GW can accurately image and locate ablation damage with different degrees of ablation, and the positioning error does not exceed 3cm, which verifies the feasibility of this method for TPS ablation damage monitoring. The research on TPS GW monitoring theory and method of hypersonic vehicle provides a reference and basis.

1 INTRODUCTION

As an advanced aircraft with both strategic deterrence and practical application capabilities, hypersonic vehicles are competing for the development of hypersonic vehicle technology by world powers, investing tens of billions of dollars [1-2]. The maximum flight Mach number during re-entry into the atmosphere can reach 20. Thermal protection structures are the key structures of hypersonic vehicle. The shock wave compression, viscous friction and other effects caused by high-speed flight cause the surface temperature of the structure to rise sharply.

The surface temperature of the nose cone and the leading edge of the wing reaches 1800~2000℃, and the temperature of the windward side of the fuselage is also around 1200℃, causing TPS to be prone to ablation, cracks, delamination, dents and other damage, which makes it safer Service leaves serious hidden dangers [3-4], so SHM is urgently needed.

In recent years, in the research on SHM technology for thermal protection structures of hypersonic vehicles, the structural damage wave imaging method based on piezoelectric sensor arrays and ultrasonic GW has gradually become a research hotspot. This method uses monitoring information from multiple guided wave excitation-sensing channels in a piezoelectric sensor array to enhance the damage effect by controlling the array synthesis mechanism. According to different imaging principles, it can be divided into delayed-and-accumulation imaging, time reversal imaging, phased array imaging, multiple signal classification imaging, etc. Among them, the time-lapse superposition imaging method is a simple and effective damage imaging method. In this method, during the regional imaging process, the amplitudes of the corresponding propagation times of the array signals are added to obtain the energy value of the imaging area, where the bright spots with larger energy correspond to the damage scattering positions. Michaels[5], Chang[6] and Qing[7] first studied the application of this method in guided wave structure health monitoring and the basic principles of its implementation. Shan[8], Cai[9,10], Hall[11] and others respectively proposed effective scattering signal extraction, linear dispersion signal construction and minimum variance distortion-free response algorithms to suppress the multi-mode and dispersion effects of GW on the delay. The influence of delayed-and-accumulation imaging can be improved to improve the accuracy of delayed-and-accumulation imaging method. Ren [12] et al. improved the delayed-and-accumulation imaging method through damage number determination, damage size classification based on probability models, and wave speed adaptive selection. They also conducted multi-damage imaging experiments on composite structures to verify it. In summary, the delayed-and-accumulation imaging method is simple and easy to implement, can monitor multiple damages, and has been initially applied to real engineering structures.

Therefore, this paper uses the delayed-and-accumulation damage imaging method based on GW to conduct damage imaging research on the ablation damage of quartz ceramic TPS structures. First, the ablation damage of the quartz ceramic TPS structure was caused by oxygen-acetylene high-temperature and high-speed airflow ablation. Secondly, a guided wave monitoring experimental method for the ablation of quartz ceramic TPS was designed, and the results of the quartz ceramic TPS under different states and different degrees of damage were obtained. GW signal, and finally by extracting the GW signal characteristics under different states and different damage degrees, the delayed-and-accumulation imaging method is used to image and locate the ablation damage of quartz ceramics.

2 GW MONITORING METHOD FOR QUARTZ CERAMICS TPS

This section mainly introduces the principle of ablation monitoring based on guided wave (GW), and secondly introduces the principle of delayed-and-accumulation damage imaging method based on GW monitoring method.

2.1 Principle of guided wave monitoring for TPS

During the high-speed flight of a hypersonic aircraft, the outer surface of the TPS is in a

high-temperature state. Currently, the existing sensors cannot work under the high-temperature state of the outer surface of the structure. Therefore, this paper proposes to arrange piezoelectric sensors in the low-temperature area of the inner surface of the TPS. monitor. Aiming at the ablation damage caused by high-temperature airflow on the outer surface of the TPS of the hypersonic aircraft, the principle of guided wave monitoring is shown in Figure 1. The piezoelectric sensor (PZT) is integrated with the low-temperature zone of the inner surface of the TPS of the aircraft. Through the piezoelectric sensor The actively excited guided wave signal is transmitted to the high temperature area on the outer surface, and then the response signal is received by the sensor network arranged in the low temperature area on the inner surface. The response signal of the outer surface of the TPS structure in a healthy state is the reference signal. The propagation characteristics of the guided wave signal will change after encountering high-temperature airflow damage on the outer surface of the TPS during the propagation process. The response signal in this damaged state is the monitoring signal. By comparing and analyzing the changes in the time domain, frequency domain, and time-frequency domain characteristics of the reference signal and the monitoring signal, such as the amplitude, phase, and energy of the signal, the high-temperature airflow damage on the outer surface of the TPS is evaluated [13-15].

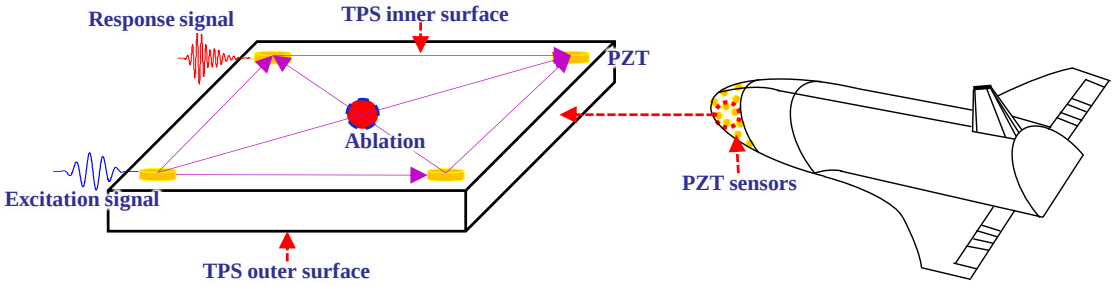

Figure 1: Principle of guided wave monitoring

2.2 Principle of delayed-and-accumulation damage imaging of TPS

The principle diagram of the delay-and-accumulation imaging algorithm is shown in Figure 2. When damage occurs in the structure, the guided wave signal is scattered during the propagation process, resulting in a damage scattering signal, which is superimposed with the direct guided wave signal. In the actual monitoring process, by monitoring Each point in the area is regarded as a potential damage location. The propagation speed of the guided wave in the structure, that is, the group velocity, is used to superimpose the wave packet amplitude of the damage scattering signal obtained by the difference, thereby obtaining a pixel map reflecting the damage location. When the corresponding point of the actual damage position is searched, the pixel value increases abnormally, thereby achieving damage location imaging.

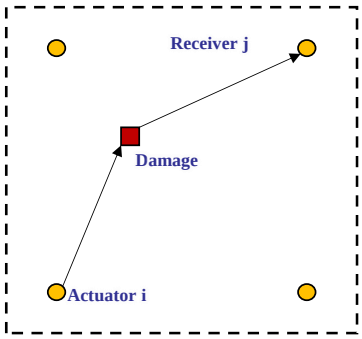

Figure 2: Schematic diagram of delayed-and-accumulation imaging algorithm

3 EXPERIMENTAL SETUP RESULTS AND ANALYSIS

This section mainly selects the quartz ceramic TPS structure, carries out the oxygen-acetylene high-temperature and high-speed airflow ablation guided wave monitoring experiment, and obtains the guided wave monitoring signals and ablation experimental results under different ablation damage states, and compares the obtained GW signals were analyzed.

3.1 Experimental specimen and sensor layout

The experimental object is a typical quartz ceramic TPS with dimensions of 250 × 250 × 30mm3, as shown in Figure 3(a), and its material parameters are shown in Table 1. Arrange 8 piezoelectric sensors, numbered 1-8, on the ablated back of the quartz ceramic structure. All sensors form 28 excitation sensing channels through non-repetitive excitation sensing, forming a 200×200mm2 monitoring area. The ablation position is the front side of the structure. The center position is shown in Figure 3(b).

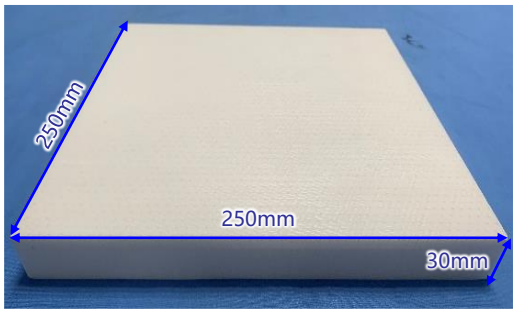

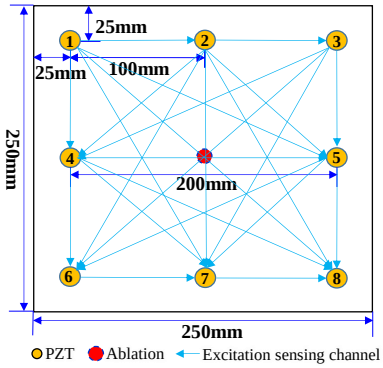

（a）Experimental specimens （b）Sensor layout and channel settings

Figure 3: Quartz ceramic physical object, sensor layout and channel settings

3.2 Experimental process and results

The experimental platform integration includes high-temperature airflow application methods and systems, guided wave signal acquisition methods and systems, and damage measurement methods. The high-temperature airflow application method of TPS adopts the

Table 1: The main material parameters of quartz ceramic

Material parameter	Value
Ablation temperature	1200 ℃
Ablation rate	0.12 mm/s
Thermal conductivity	≤0.75 W/m • K
Bending strength	≥45 Mpa
Tensile strength	≥30 Mpa
Elasticity modulus	10~15 Gpa
Density	1.70~1.75 g/cm^3

oxygen-acetylene ablation experimental method specified in GJB 323B-2018 "Ablation Test Methods for Ablative Materials" [16]. The oxygen-acetylene ablation and guided wave monitoring experimental platform is shown in Figure 4(a). The entire experimental platform consists of a specimen fixture, an ablation gun, and an ablation console. The TPS is clamped by the fixture, and the ablation gun is responsible for The high-temperature flame is sprayed to ablate the TPS. The ablation console mainly controls the ablation time, fuel ratio and mechanical operation of the ablation gun. In terms of monitoring system, the integrated guided wave SHM system [17] (referred to as: guided wave monitoring system) independently developed by Nanjing University of Aeronautics and Astronautics is used, as shown in Figure 4(a). At the same time, the system controls 2 of the 8 sensors to apply the guided wave excitation signal and obtain the response signal. By scanning 28 guided wave excitation-sensor network channels composed of 8 sensors, Acquire guided wave signals covering the entire structure monitoring area.

Before applying high-temperature airflow ablation to the TPS, the guided wave monitoring system acquires the reference signal of the TPS in a healthy state, represented by H, and measures the initial depth of the TPS ablation location. High-temperature airflow ablation is then applied to the TPS. A complete ablation process includes three parts: ignition, ablation, and flameout. As shown in Figure 4(b), the ablation duration is set to 20s.

For each ablation, the experimental process is designed as follows: the ablation gun is ignited, and the ablation heat flux density of the console is adjusted to 3700KW/m2; the ablation gun is rotated to apply high-temperature airflow to the TPS, and the temperature is measured during the TPS ablation process; the ablation gun After turning off the flame, when the overall temperature of the TPS drops to near the initial temperature point, the guided wave signal is acquired, and the damage depth at the center point of the ablation position is measured. In the study, a total of 18 ablations were applied to TPS, and the guided wave signal obtained after each ablation is represented by Dn, where n=1, 2,...,18.

In the above experiment, the parameters of the guided wave monitoring system are set as follows: the excitation signal waveform is sinusoidal modulation with 5 peaks, the center frequency of the excitation signal is swept from 50kHz to 300kHz, the frequency interval is 10kHz, the excitation signal amplitude is ±70V; guided wave response signal sampling The rate is 10MSamples/s, the sampling length is 5000 data points, the pre-trigger acquisition mode is used, and the trigger length is 500 data points.

（a）Ablation experimental platform （b）Ablation experiment process

Figure 4: Guided wave monitoring experimental platform for ablation and ablation experimental process

During the ablation process, the depth and width of the ablation damage of quartz ceramic TPS were statistically calculated. It was found that as the ablation degree increased, the damage morphology gradually transformed from point-like pits to bowl-shaped pits. The measurement results of damage depth and width are shown in Figure 5. As the number of ablation increases, the damage depth shows a linear increase trend, and the damage width increases linearly in the early stage and becomes stable in the later stage.

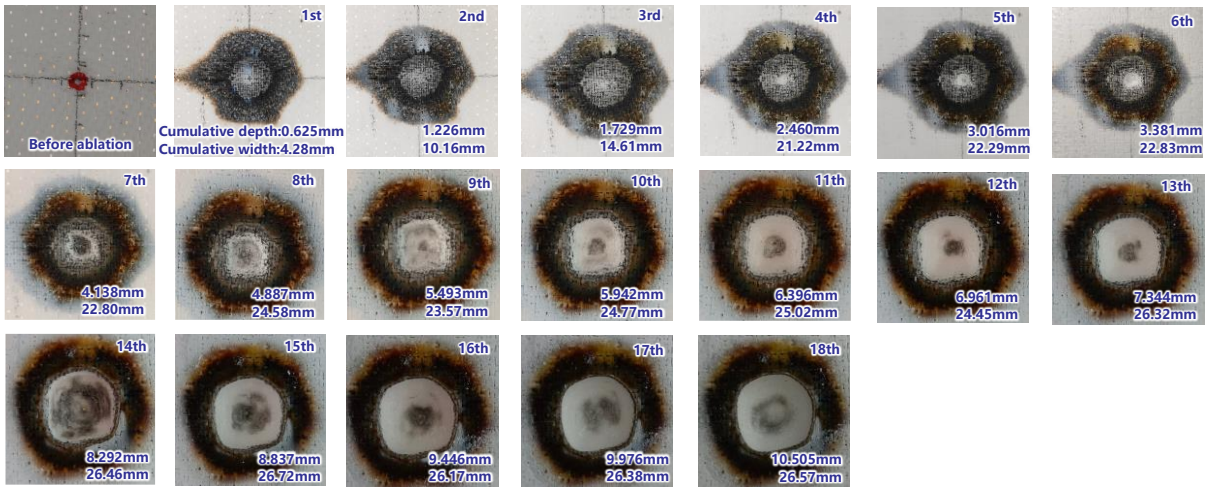

Figure 5: Measurement results of ablation morphology, ablation depth and ablation width of quartz ceramic before ablation and after 18 ablation experiments

3.3 Optimal frequency selection and typical guided wave signals

For the GW monitoring signal of quartz ceramic TPS, the signal frequency that is more sensitive to damage can be obtained by drawing the waterfall chart of the signal at different frequencies. Figure 6 shows the signal waterfall diagram of the two excitation sensing channels longitudinal 2-7 and transverse 4-5 in the full frequency range of 50~300kHz when TPS is not ablated. It can be seen from the waterfall chart that the GW on the quartz ceramic TPS can be excited and respond normally. According to the principle that the direct wave pattern is clear and the amplitude is large, the direct wave signal of 100kHz is the optimal frequency for analysis.

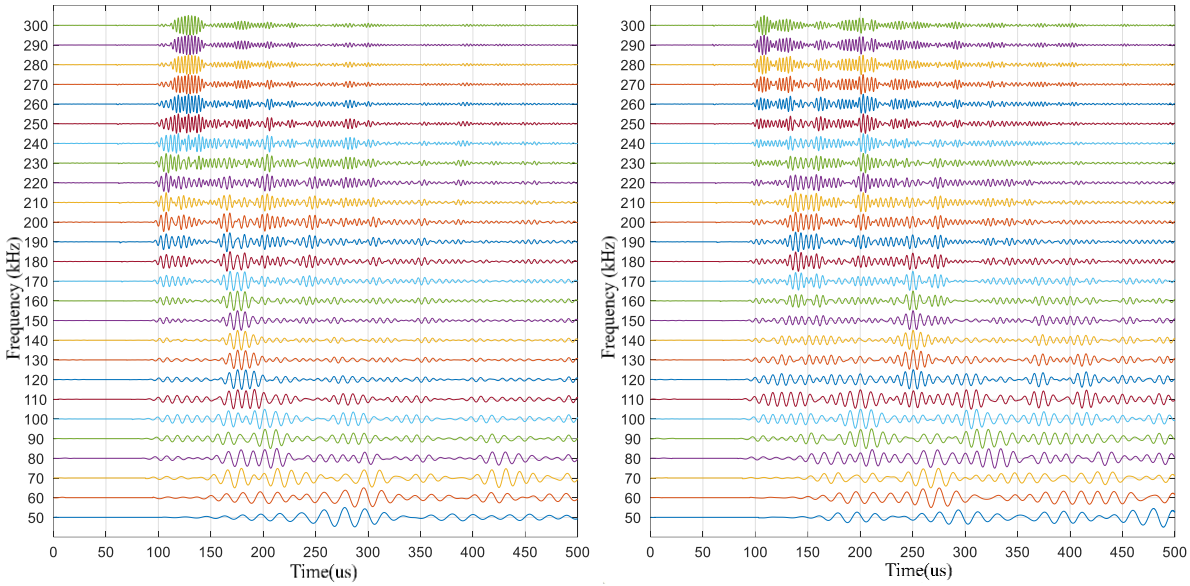

(a) Channel 4-5 (b) Channel 2-7

Figure 6: The frequency sweeps GW signals from 50 to 300 kHz.

The reference signals of channels 4-5 that directly pass through the ablation damage and the 1-3 channels that are far away from the ablation damage are obtained through comparative analysis, as well as the monitoring signals after 18 times of ablation. The signal center frequency is 100kHz, and the signal is as shown in the figure 7 and Figure 8. As can be seen from the figure, the GW signal after TPS ablation has obvious changes. It can be seen from the difference signal between the reference signal and the monitoring signal given in Figure 7(b) and Figure 8(b) that the amplitude of the difference signal in the damaged channel is more than 20 times that of the channel away from the damage, and the difference The amplitude of the signal increases with the degree of ablation. It shows that the guided wave monitoring method can effectively monitor ablation damage and characterize the severity of ablation damage.

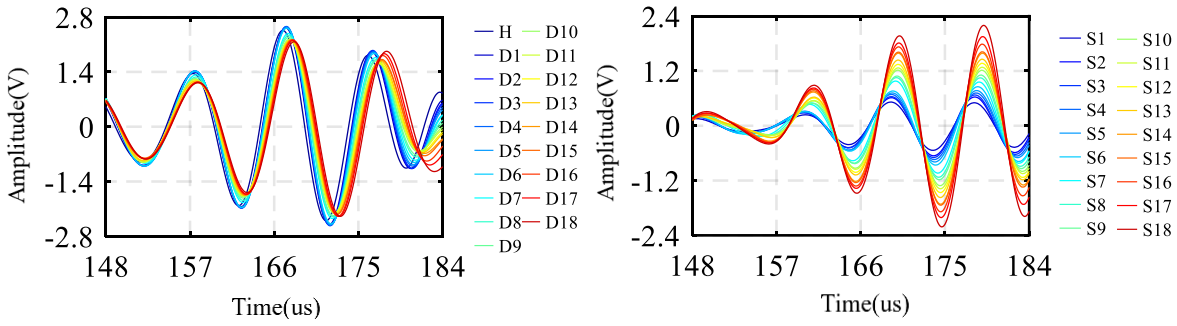

(a) Baseline and Monitor Signals (b) Scattering signals

Figure 7: The reference signal and monitoring signal collected before and after 18 ablation of channels 4-5, and the difference signal between the reference signal and monitoring signal of the corresponding channel.

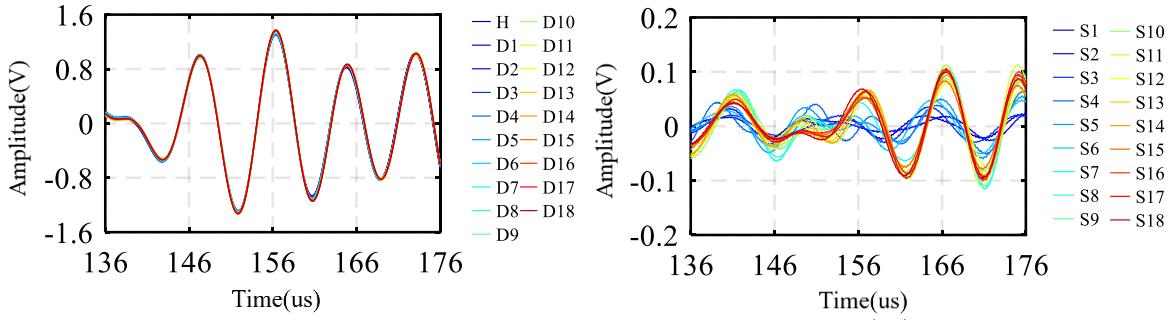

(a) Baseline and Monitor Signals (b) Scattering signals

Figure 8: The reference signal and monitoring signal collected before and after 18 ablation of channels 1-3, and the difference signal between the reference signal and monitoring signal of the corresponding channel.

4 DELAY-AND-ACCUMULATION IMAGING METHOD

The delay-and-accumulation imaging method used in this section processes the guided wave signal to create an image of the ablation damage area. First, the process of the ablation damage delayed accumulation imaging algorithm is introduced. Secondly, this method is used to delay and accumulate the GW signal. Monitor the location and extent of ablation damage.

4.1 Delayed-and-accumulation imaging process of quartz ceramic TPS ablation

Aiming at the ablation damage of quartz ceramic TPS, the basic process of ablation damage monitoring of its delayed-and-accumulation imaging algorithm is shown in Figure 9. The specific algorithm process is as follows:

(1) First, divide the entire ablation monitoring area into multiple pixels at equal intervals, and the X and Y directions are divided into 200 equal parts. The larger the value, the clearer the imaging result, but the greater the calculation amount of the algorithm. The position of each pixel is expressed by its coordinates (x, y) in the monitoring area, see formula (2-1), where x_{min} and x_{max} respectively represent the minimum and maximum values of the X coordinates of all sensors; y_{min} and y_{max} respectively Represents the minimum and maximum values of the Y coordinates of all sensors.

$$\begin{cases} x = x_{\min} + (m-1) \times \dfrac{x_{\max} - x_{\min}}{200} \\ y = y_{\min} + (m-1) \times \dfrac{y_{\max} - y_{\min}}{200} \end{cases} \tag{1}$$

(2) Then, the health signal and damage signal of each excitation sensing channel are differenced to obtain the damage scattering signal of each channel, and the signal envelope Eij of each channel is obtained through wavelet transformation. Here, Shannon complex wavelet transform is used.

(3) Calculate the expected arrival time of the damage scattering signal of each pixel on each channel, see formula (2-2). Where c is the average velocity of all channels, toff is the time offset corresponding to the excitation signal, (x_i, y_i) are the coordinates of the i-j channel excitation element, (x_j, y_j) are the coordinates of the i-j channel sensing element.

$$t_{ij}(x,y) = t_{off} + \frac{r_i + r_j}{c} = t_{off} + \frac{\sqrt{(x-x_i)^2 + (y-y_i)^2} + \sqrt{(x-x_j)^2 + (y-y_j)^2}}{c} \quad (2)$$

(4) Calculate the pixel value of each point in the ablation monitoring area separately. The pixel value of each point is accumulated by the corresponding value $E_{ij}(t_{ij}(x,y))$ of the point in the damage scattering signal envelope E_{ij} of each channel. It is assumed that there are N channels in total.

$$E(x,y) = \sum_{i=1}^{N-1} \sum_{j=i+1}^{N} E_{ij}(t_{ij}(x,y)) \quad (3)$$

(5) The largest point among all pixel values will be searched to determine whether there is damage in the structure. If the maximum value of the pixel is less than the damage threshold, it will be determined that there is no ablation damage in the structure. All pixel values will be set to zero for imaging and output cloud map. If the pixel If the maximum value is greater than the damage threshold, it is determined that there is ablation damage in the structure, and the original pixel value is retained for imaging and output cloud image, and the coordinates of the point with the maximum pixel value in the image are searched as the final ablation damage determination position.

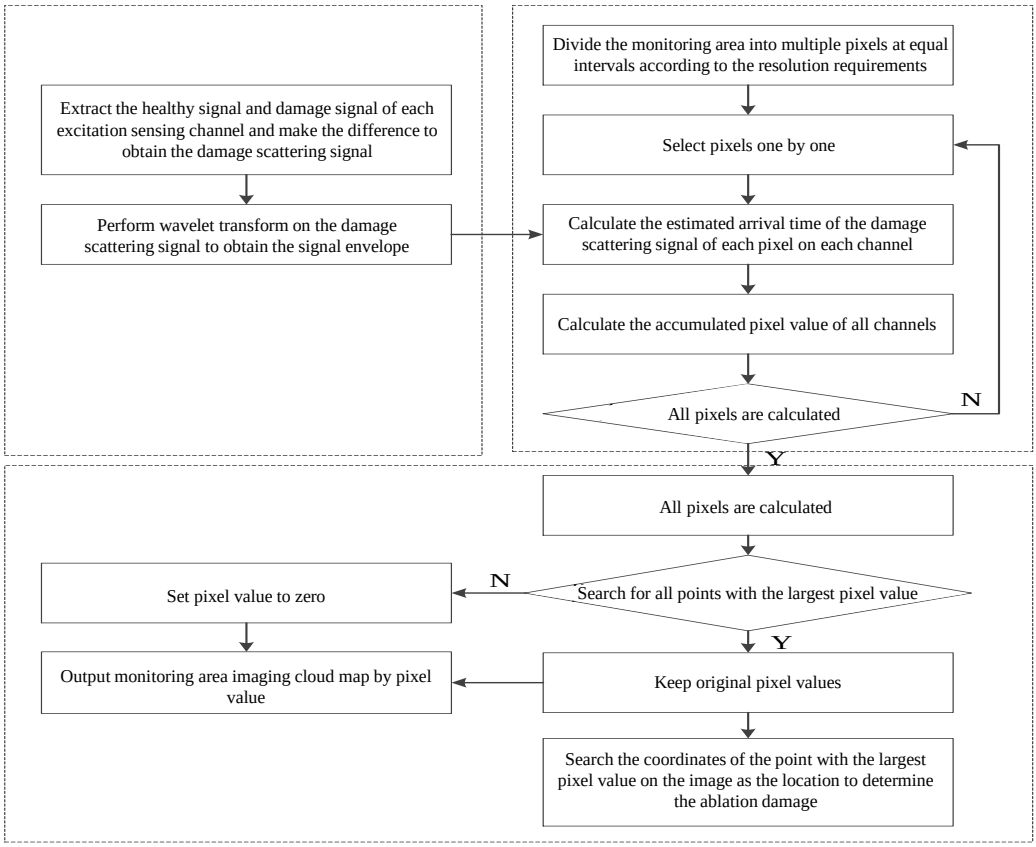

Figure 9: Delayed-and-accumulation imaging algorithm flow

4.2 Delayed-and-accumulation imaging results of quartz ceramic TPS ablation

According to the principle of delayed-and-accumulation imaging algorithm in Section 2.2, this paper selects 28 non-repeating channels composed of 8 sensors of quartz ceramic TPS structure to carry out delayed-and-accumulation imaging of ablation damage. The imaging detection area is 200×200mm^2. According to Section 4.1 The quartz ceramic ablation damage delayed-and-accumulation imaging algorithm process, the delayed-and-accumulation imaging results and positioning error of ablation damage after 18 ablations are shown in Figure 10. The damage positioning is accurate and the error does not exceed 3cm, which is basically consistent with the damage location. At the same time, the maximum pixel value in the monitoring area after each ablation was counted. The results are shown in Figure 11. It was found that the maximum pixel value increased with the increase in the degree of ablation. The results show that the delayed-and-accumulation imaging algorithm can be used for quartz ceramic TPS. The ablation damage can be accurately located, and the severity of the ablation damage can be characterized by the pixel value.

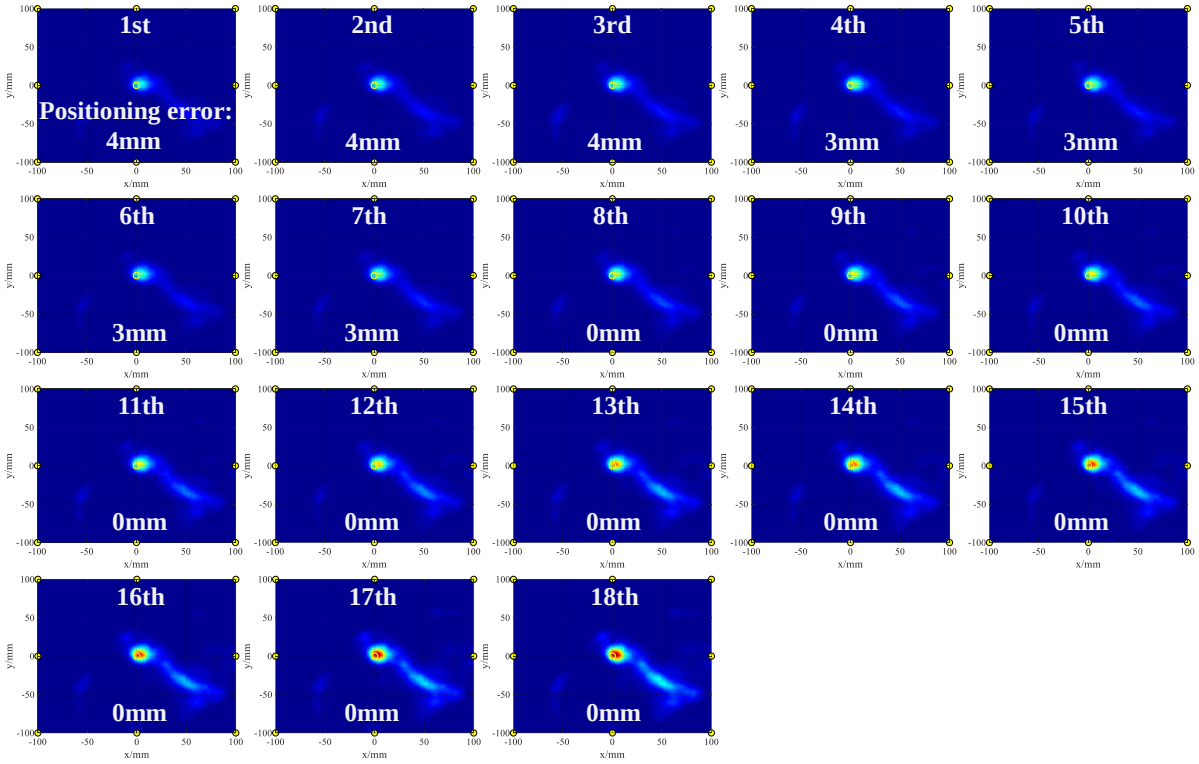

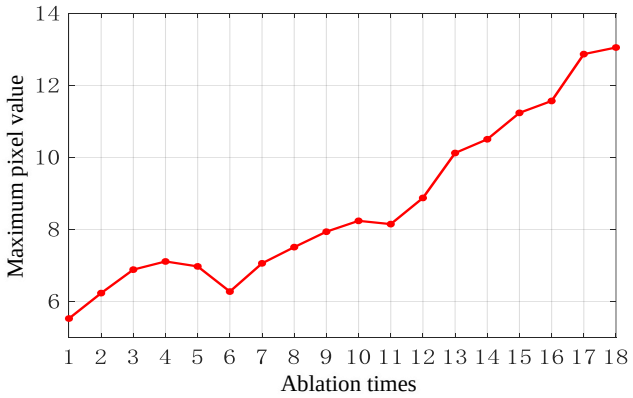

Figure 11: The maximum pixel value of the center point of delayed accumulation imaging changes with the number of ablation times

5 CONCLUSION

In this research work, this paper successfully employed GW and the delay-and-accumulation imaging method to assess ablation damage in quartz ceramic TPS structures for hypersonic vehicles. Our findings highlight the potential of this approach for real-time monitoring of TPS integrity during reentry. The accuracy of the method in imaging and locating damage, even with varying degrees of ablation, underscores its practical applicability. This research lays the groundwork for TPS guided wave monitoring theory and methods, offering valuable insights for the development of advanced SHM systems for hypersonic vehicles.

ACKNOWLEDGMENTS

This work is sponsored by National Natural Science Foundation of China (Grant No. 52275153, Grant No.51975292), Fundamental Research Funds for the Central Universities (Grant No. NI2023001), Outstanding Youth Foundation of Jiangsu Province of China No. BK20211519, Research Fund of State Key Laboratory of Mechanics and Control of Mechanical Structures (Nanjing University of Aeronautics and Astronautics) (Grant No. MCMS-I-0521K01), Fundamental Research Funds for the Central Universities (Grant No. 1001-XAC21022), Priority Academic Program Development of Jiangsu Higher Education Institutions of China.

REFERENCES

[1] SZIROCZAK D, SMITH H. A review of design issues specific to hypersonic flight vehicles[J]. Progress in Aerospace Sciences, 2016, 84(1): 1-28.

[2] UYANNA O, NAJAFI H. Thermal protection systems for space vehicles: A review on technology development, current challenges and future prospects[J]. Acta Astron- autica, 2020, 176: 341-356.

[3] DARYABEIGI K. Thermal analysis and design optim-ization of multilayer insulation for reentry aerodynamic heating[J]. Journal of Spacecraft and Rockets, 2002, 39(4): 509-514.

[4] XIE W H, HAN G K, MENG S H, et al. Development status and trend of thermal protection structure for return capsules and space probes[J]. Acta Aeronautica et Aetronautica Sinica,

2019, 40(8): 022792.
[5] Michaels, Jennifer E. Detection, localization and characterization of damage in plates with an in situ array of spatially distributed ultrasonic sensors. Smart Materials and Structures, 2008, 17(3): 035015.
[6] Ihn J B, Chang F K. Pitch-catch active sensing methods in structural health monitoring for aircraft structures. Structural Health Monitoring, 2008, 7(1): 5-19.
[7] Qing X P, Beard S J, Kumar A, et al. Advances in the development of built-in diagnostic system for filament wound composite structures. Composites science and technology, 2006, 66(11-12): 1694-1702.
[8] Shan S B, Qiu J H, Zhang C, et al. Multi-damage localization on large complex structures through an extended delay-and-sum based method. Structural Health Monitoring, 2016, 15(1): 50-64.
[9] Cai J, Yuan S F, Qing X P, et al. Linearly dispersive signal construction of Lamb waves with measured relative wavenumber curves. Sensors and Actuators A: Physical, 2015, 221: 41-52.
[10] Cai J, Yuan S F, Wang T G. Signal construction-based dispersion compensation of lamb waves considering signal waveform and amplitude spectrum preservation. Materials, 2017, 10(1): 4.
[11] Hall J S, Michaels J E. Multipath ultrasonic guided wave imaging in complex structures. Structural Health Monitoring, 2015, 14(4): 345-358.
[12] Ren Y Q, Qiu L, Yuan S F, et al. Gaussian mixture model and delay-and-sum based 4D imaging of damage in aircraft composite structures under time-varying conditions. Mechanical Systems and Signal Processing, 2020, 135:106390.
[13] IHN J B, CHANG F K. Detection and monitoring of hidden fatigue crack growth using a built-in piezoelectric sensor/actuator network: I. Diagnostics[J]. Smart Material Structures, 2004, 13(3): 609-620.
[14] CHO H, LISSENDEN C J. Structural health monitoring of fatigue crack growth in plate structures with ultrasonic guided waves[J]. Structural Health Monitoring, 2012, 11(4): 393-404.
[15] CHEN J, YUAN S F, JIN, X. On-line prognosis of fatigue cracking via a regularized particle filter and guided wave monitoring. Mechanical Systems and Signal Processing, 2019, 131: 1-17.
[16] HE P, WANG L L, MO J A, et al. Test method for abla-tion of ablators: GJB 323B-2018[S]. Beijing: Military Standard Press of Commission of Science, Technology and Industry for National Defense, 2018.
[17] QIU L, YUAN S F, WANG Q, et al. Design and Experi- ment of PZT Network-based Structural Health Monitor-ing Scanning System[J]. Chinese Journal of Aeronautics, 2009, 22(5): 505-512.